pH-Dependent Conformational Change of Gastric Mucin Leads to Sol-Gel Transition

Xingxiang Cao,*# Rama Bansil,§ K. Ramakrishnan Bhaskar,¶ Bradley S. Turner,¶ J. Thomas LaMont,¶ Niu Niu,# and Nezam H. Afdhal#

*Department of Chemistry, Boston University, Boston, Massachusetts 02215; #Section of Gastroenterology, Boston Medical Center, Boston, Massachusetts 02218; §Department of Physics, Boston University, Boston, Massachusetts 02215; and ¶Department of Medicine, Beth Israel Deaconess Medical Center and Harvard Medical School, Boston, Massachusetts 02215 USA

ABSTRACT   We present dynamic light scattering (DLS) and hydrophobic dye-binding data in an effort to elucidate a molecular mechanism for the ability of gastric mucin to form a gel at low pH, which is crucial to the barrier function of gastric mucus. DLS measurements of dilute mucin solutions were not indicative of intermolecular association, yet there was a steady fall in the measured diffusion coefficient with decreasing pH, suggesting an apparent increase in size. Taken together with the observed rise in depolarized scattering ratio with decreasing pH, these results suggest that gastric mucin undergoes a conformational change from a random coil at pH $\geq$ 4 to an anisotropic, extended conformation at pH $<$ 4. The increased binding of mucin to hydrophobic fluorescent with decreasing pH indicates that the change to an extended conformation is accompanied by exposure of hydrophobic binding sites. In concentrated mucin solutions, the structure factor $S(q, t)$ derived from DLS measurements changed from a stretched exponential decay at pH 7 to a power-law decay at pH 2, which is characteristic of a sol-gel transition. We propose that the conformational change facilitates cross-links among mucin macromolecules through hydrophobic interactions at low pH, which in turn leads to a sol-gel transition when the mucin solution is sufficiently concentrated.

INTRODUCTION

Mucins are high molecular weight ($>10^6$) glycoproteins contained in the mucosal secretions covering epithelial cell surfaces and are primarily responsible for the protective properties of the viscoelastic mucous barrier (Bansil et al., 1995). This protective function is particularly critical in the stomach: the pH of the lumen is between 1 and 2, yet the gastric epithelium remains undamaged. It is generally believed that the gelation of gastric mucin provides this protection, even though the phase behavior of the mucus layer is not clear and the actual mechanism of the gelation is not fully understood (Hollander, 1954; Heatley, 1959; Allen and Garner, 1980; Williams and Turnberg, 1980; Allen, 1981; Pfeiffer, 1981; Bell et al., 1982; Strous and Dekker, 1992).

We have previously reported that solutions of pig gastric mucin (PGM) undergo a marked increase in viscosity at low pH, and protein-protein interactions are responsible for this viscosity increase (Bhaskar et al., 1991). In earlier, in vitro studies of HCl injected into PGM solutions (Bhaskar et al., 1992), we observed narrow channels of the acid when the pH of the PGM solution was 5 or greater, while HCl was unable to penetrate when the pH of the PGM solutions was below pH 4. Such observations offer a plausible explanation for how secreted acid reaches the gastric lumen without

disrupting the mucus layer, and how the acid is prevented from diffusing back to damage the epithelium. These pH-dependent properties were found to be completely reversible, suggesting that PGM solution's phase behavior at different pH values might be directly responsible for gastric mucin's protection function.

In order to examine whether a sol-gel transition occurs in gastric mucin we have adopted an approach similar to that used in studying sol-gel transitions in synthetic gels using dynamic light scattering (DLS). Normally, a linear polymer solution or monodisperse colloidal particle suspension exhibits an exponential decay in the intensity autocorrelation function, which broadens if there is polydispersity (Berne and Pecora, 1976; Chu, 1991; Brown and Nicolai, 1993). The situation becomes more complicated when the polymers are branched or the particles aggregate to form clusters. Several DLS studies on synthetic gels in organic solvents (Adam et al., 1988; Martin and Wilcoxon, 1988; Martin et al., 1991; Fang et al., 1991; Konak et al., 1996) and naturally occurring biopolymer gels in water (Nystrom and Lindman, 1995) show that in the vicinity of a sol-gel transition the long-term decay of the correlation function changes from a stretched exponential correlation function in pre-gel solutions to a power-law on the post-gel side. The stretched exponential behavior reflects that in the immediate vicinity of the gel point the cluster size distribution in a pre-gel solution is extremely polydisperse, and the dynamics of the partially penetrating clusters is coupled. In addition to this diffusion of coupled clusters, a semidilute solution also has a cooperative diffusion mode that arises from the collective dynamics of the concentration fluctuations corresponding to the fluctuations in the correlation length of

the semidilute solution (Brown and Nicolai, 1993). This cooperative or collective mode can be well described by a single exponential decay and is much faster than the diffusive dynamics of the coupled clusters. Consequently, the correlation function can be written as the sum of a single exponential decay and a stretched exponential decaying part.

On the post-gel side, in the vicinity of the sol-gel transition, the mode corresponding to cluster dynamics becomes a power-law, as the relaxation spectrum does not exhibit any characteristic time scale. This long-term power law relaxation is only significant in the immediate vicinity of the gel point, where an incipient percolating, fractal cluster is first formed. As gelation proceeds beyond the gel point the formation of additional cross-links leads to a gel that is no longer dominated by a fractal cluster. Such a well-gelled sample exhibits a dominant collective diffusion mode, which is single-exponential in character and represents the dynamics of the concentration fluctuations occurring on a length scale of the correlation length in the gel (Tanaka et al., 1973). Since the correlation length is typically much smaller than the characteristic size of the percolating cluster, the collective mode is much faster than the slow power-law dynamics associated with the percolating cluster. Thus the functional form of the long-term decay of the correlation function is a signature of the state of aggregation/gelation of the sample.

We undertook the present study of dynamic light scattering and hydrophobic binding to examine the influence of pH on the structure-function characteristics of PGM solution as well as the PGM macromolecule itself, and to identify whether the solution's and macromolecule's behaviors at different pH values are correlated. A model for the stomach's protection mechanism at the molecular level is proposed.

MATERIALS AND METHODS

Isolation and purification of mucins

PGM and bovine gallbladder mucin (GBM) were isolated and purified from mucosal scrapings of pig stomach epithelium and bovine gallbladder epithelium, respectively, by gel filtration followed by density gradient ultracentrifugation in CsCl using the general methods described previously (Smith and LaMont, 1984; Gong et al., 1990). Purified mucins were shown to be free of lipids, low molecular weight protein, and glycoprotein contaminants (Gong et al., 1990). Except where stated otherwise, mucin solutions were prepared by dissolving mucin in 10 mM sodium phosphate buffer. Aqueous HCl was used to adjust the pH of the solution to the desired value.

Hydrophobic dye-binding studies

The negatively charged 1-anilino-8-naphthalene sulfonate (ANS) and the uncharged N-phenyl-1-anphthyl amine (NPNA) were used as fluorescent probes in the hydrophobic binding studies. Fluorescence measurements were carried out using a Perkin-Elmer LS-5B luminescence spectrometer, equipped with a four-position thermostatically controlled turret cell holder. Solutions of the fluorescence probe were prepared fresh before measurements. ANS was prepared as an aqueous solution of ~1 mg/ml and diluted as needed. Because of its limited solubility, solutions of NPNA were prepared in 60 mM HCl in 50% ethanol at a concentration of 1 mM. Excitation wavelengths of 365 and 342 nm were used for studies with ANS and NPNA, respectively. For temperature-dependent studies, the prepared solutions were placed in the cell holder and water at the lowest desired temperature was circulated for a period of ~30 min. The actual temperature of the test solution was checked using a thermometer before making the measurements. The circulating bath was set to progressively higher temperatures and the measurements were made as before. The fluorescence values were found to be quite stable over the period of measurements. PGM solutions of different concentrations and pH values ranging from 2 to 7 were incubated with the fluorescent probe.

Dynamic light scattering studies

DLS measurements were made with an argon laser (λ = 514.5 nm), a variable-scattering angle goniometer (Brookhaven Instruments, Holtsville, NY), and a Brookhaven Instruments 9000 autocorrelator. The sample cell was placed in a thermostatted glass vat with optically flat windows filled with toluene to match the refractive index of the glass containers. All experiments were carried at 37.0 ± 0.1°C. The light scattered at a fixed angle θ was collected by a photo tube via a fiber optic cable using optics mounted on the goniometer's rotating arm. With this instrument it was possible to cover an angular range of 30–130°, which corresponds to a range of 0.84–2.9 × 10^7 m^{-1} for the scattering vector q, where $q = (4\pi n/\lambda)\sin(\theta/2)$ with n the refractive index of the solvent.

For depolarized measurements, two Glan-Thompson polarizers (extinction ratio < 10^{-7}) were used as polarizer to produce vertically (V) polarized incident light, and as analyzer to detect either horizontally (H) or vertically (V) polarized scattered light. In addition to the depolarized dynamic light scattering (DDLS) measurements, we also obtained the depolarization ratio $\rho = I_{VH}/I_{VV}$ at θ = 90°, where I_{VH} and I_{VV} are the respective depolarized and polarized scattered intensities.

DLS data analysis

For DLS data analysis, the dynamic structure factor $S(q, t)$ of the scattered electric field was obtained from the normalized intensity autocorrelation function $G_2(t)$ measured by DLS:

$$S(q, t) = [(G_2(t) - B)/(G_2(0) - B)]^{0.5}, \qquad (1)$$

where B is the baseline of the measurement. As is well known, in a monodisperse solution of macromolecules or particles, $S(q, t)$ decays exponentially (Berne and Pecora, 1976). In general, however, with a dilute or semidilute polymeric solution of noninteracting linear polymers, polydispersity and the possibility of more than one diffusive mode lead to a broad distribution of exponentials (Chu, 1991; Brown and Nicolai, 1993) so that

$$S(q, t) = \int A(\tau)\exp(-q^2t/\tau)d\tau. \qquad (2)$$

Here $A(\tau)$ denotes the relative contribution of the mode with characteristic decay time τ to the correlation function and was determined by a Laplace inversion technique, known as CONTIN (Provencher et al., 1978). The diffusion coefficient D and decay rate Γ are related to the characteristic decay time τ by

$$\Gamma = Dq^2 = 1/\tau. \qquad (3)$$

As discussed earlier, in the immediate vicinity of the gel point in the pre-gel state the correlation function exhibits a stretched exponential decay. Thus $S(q, t)$ was fit to the sum of a single-exponential decay and a stretched exponential decay,

$$S(q, t) = A_c\exp(-\Gamma_c t) + A_s\exp(-[\Gamma_s t]^\beta). \qquad (4)$$

Here Γ_i (i = c or s) is the characteristic decay rate: c is the fast, cooperative decay mode, s is the slow decay mode attributed to the coupled dynamics of the polydisperse clusters/aggregates, and A_i (i = c or s) is the relative scattering amplitude. The exponent β is related to the width of the corresponding distributions of the decay rate Γ_s; the smaller the value of β, the broader the distribution (Martin et al., 1991). At short times the collective mode dominates, whereas at long times the stretched exponential tail dominates.

In gels, just above the sol-gel transition the mode corresponding to cluster dynamics becomes a power-law. Thus, at sufficiently long decay time t, $S(q, t)$ can be expressed as

$$S(q, t) \sim t^{-\Phi} \tag{5}$$

i.e., a plot of $\log[S(q, t)]$ against $\log(t)$ yields a straight line with $-\Phi$ as the slope, if the system in question is in the vicinity of a sol-gel transition.

In DDLS measurements, the decay rate Γ_{VH} was obtained by analyzing $S_{VH}(q, t)$ with the CONTIN program (Provencher et al., 1978).The decay rate Γ_{VH} is related to the translational and rotational diffusion coefficients, D and D_R respectively, by

$$\Gamma_{VH} = Dq^2 + 6D_R. \tag{6}$$

By measuring DDLS at different scattering angles, a linear fit of Γ_{VH} versus q^2 yields D and D_R. The dimensions of the macromolecules were calculated from theoretical models that give the dependence of the translational and rotational diffusion constants of rods and wormlike chains on structural parameters characterizing the worm (Yamakawa, 1971; Yamakawa and Fujii, 1973) or rod (Riseman and Kirkwood, 1950). Further details of these calculations are reported in the Ph.D. dissertation of one of the authors (Cao, 1997).

RESULTS AND DISCUSSION

DLS studies in dilute solutions

DLS measurements were performed on PGM solutions at different concentrations and pH values. In the following we first discuss the results in dilute solution at concentrations ≤5.0 mg/ml. Fig. 1 A shows the time dependence of the dynamic structure factor [$S(q, t)$] for PGM solution at 2.0 mg/ml and pH 7.0 over almost five decades of time delay. In Fig. 1 B we show the distribution of characteristic decay times $A(\tau)$ obtained by the Laplace inversion program of CONTIN (Provencher et al., 1978). It is clear from Fig. 1 B that in this dilute solution of mucin the dynamics is characterized by one dominant broad distribution of single-exponential decays. The two small peaks at very short and very long times, respectively, represent the after-pulsing of the photomultiplier tube at times less than a few microseconds and residual dust and small amounts of poorly dissolved material that might remain in the mucin solutions. The position of the dominant peak in the distribution of relaxation times (Fig. 1 B) was used to calculate the average decay rate Γ (see Eq. 3). Similar results were obtained by the CONTIN analysis of correlation functions measured at different angles (Cao, 1997). The decay rates for different scattering angles plotted against q^2 gave a straight line with zero intercept. This confirms that the dominant peak of the distribution shown in Fig. 1 B represents diffusive motions. The slope of the Γ versus q^2 straight line was used to calculate the average diffusion coefficient, D.
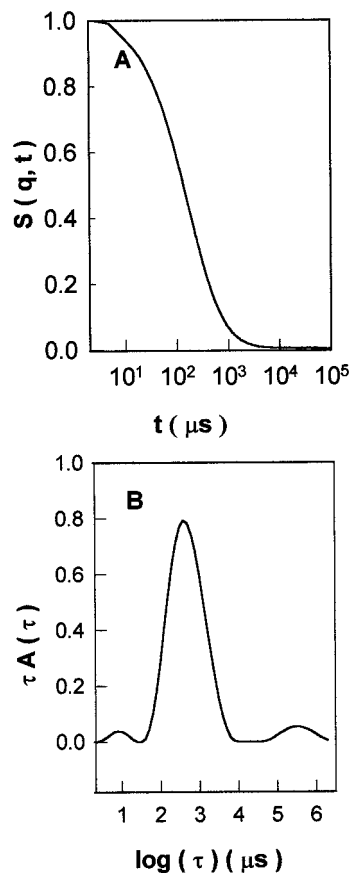

FIGURE 1 (*A*) Plot of the dynamic structure factor, $S(q, t)$ versus time t, for PGM solution of 2.0 mg/ml, pH 7.0 measured at scattering angle of 90°. (*B*) Distribution of relaxation times $A(\tau)$ obtained by Laplace inversion of the dynamic structure factor shown above, plotted as a function of the characteristic relaxation time τ. The dominant peak represents the diffusion of mucin macromolecules in the PGM solution.

Measurements of $S(q, t)$ by DLS for PGM solutions at concentrations ≤5.0 mg/ml showed similar behavior, with one dominant diffusive mode, regardless of pH and scattering angle. This implies that at concentrations ≤5.0 mg/ml PGM exists predominantly as nonassociated macromolecular species in dilute to semidilute solution. For PGM at 5.0 mg/ml, pH 7.0, $D = 7.5 \times 10^{-8}$ cm^2/s. Using the Stokes-Einstein relation,

$$R_H = \frac{kT}{6\pi\eta D}, \tag{7}$$

the hydrodynamic radius R_H for PGM is found to be $R_H = 44$ nm, which compares well with the size estimated from sedimentation data and that seen in transmission electron microscopy studies, $R = 25–75$ nm (Fiebrig et al., 1995).

pH dependence of diffusion coefficient in dilute solutions

The diffusion coefficient, D, for PGM solution of 5.0 mg/ml at different pH values is shown in Fig. 2. Clearly, there is a
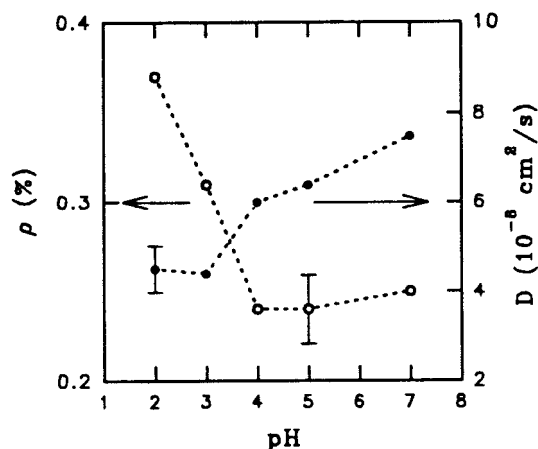
FIGURE 2 pH dependence of diffusion coefficient D (●) and depolarized scattering ratio ρ (○), of PGM macromolecules in solution of 5.0 mg/ml. A typical error bar (based on seven repeated measurements) shows the uncertainty of the D and ρ measurements. The dashed lines are drawn to guide the eye.
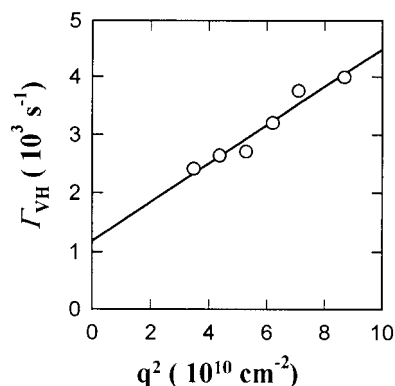

FIGURE 3 The q-dependence of the depolarized decay rate, Γ_{VH}, obtained in DDLS experiments on 5 mg/ml solution of PGM at pH 2. The non-zero intercept of the straight line fit to the data provides clear evidence of a rotational diffusion process in PGM solution at pH 2.

gradual decrease in D with decreasing pH. According to the Stokes-Einstein relation, this decrease in D corresponds to an increase in R_H.

An increase of R_H could be caused either by aggregation of PGM macromolecules or by a change in their conformation to make the overall R_H larger. Since $S(q, t)$ functions for all measurements at concentrations ≤5.0 mg/ml are broad exponential decays with one dominant mode, it can be concluded that PGM macromolecules do not aggregate at concentrations ≤5.0 mg/ml, regardless of the solution's pH. Fig. 2 also shows that the fall in D values with decreasing pH is accompanied by a sharp rise in the depolarized scattering ratio, ρ, below pH 4. The high value of ρ at low pH implies an increase in the molecular anisotropy, whereas the low value of ρ implies that PGM is in an isotropic, random-coil conformation above pH 4. The hydrodynamic radius $R_H = 44$ nm obtained from D at pH 7 lies within the range of values reported for other mucins (Bansil et al., 1995; Carlstedt et al., 1983). Therefore, both polarized and depolarized scattering results suggest that PGM undergoes a pH-dependent conformational change from an isotropic random-coil above pH 4 to a more anisotropic conformation below pH 4.

Depolarized dynamic light scattering

The depolarized scattering intensity for PGM solution at low pH was sufficiently high so that it was possible to obtain good-quality DDLS measurements. The depolarized dynamic structure factor, $S_{VH}(q, t)$, measured for PGM solution of 5.0 mg/ml at pH 2.0 were analyzed by the CONTIN program to obtain the average decay rate, Γ_{VH}. Fig. 3 shows the q-dependence of Γ_{VH}. Using Eq. 6, a linear fit of Γ_{VH} versus q^2 yields $D = 3.3 \times 10^{-8}$ cm^2/s and $D_R = 200$ s^{-1}. The D value obtained by DDLS is comparable, within error bars (see Fig. 2) to that obtained through DLS

for the same solution, $D = 4.5 \times 10^{-8}$ cm^2/s. Differences between D obtained from DLS and DDLS are also exaggerated by the fact that the DDLS measurements are done with a weaker total scattered intensity, and thus do not have the same signal-to-noise ratio. From D and D_R we can calculate the dimensions of PGM molecule in its anisotropic conformation.

Earlier light scattering studies of a variety of mucins have revealed that mucins behave as somewhat stiff, expanded random coils in solution (Carlstedt et al., 1983; Shogren et al., 1989). A wormlike chain model provides a reasonable description of the mucin chain because light scattering data analyzed using this model and calculations based on the rotational isomeric state model give similar values of molecular parameters, such as the helix pitch and persistence length (Shogren et al., 1989). For a wormlike chain (Yamakawa and Fujii, 1973), give

$$D = \frac{kT}{3\pi\eta L_c} (A_1\Lambda^{1/2} + A_2 + A_3\Lambda^{-1/2} + A_4\Lambda^{-1} + \Lambda^{-3/2}),$$
(8)

where L_c is the contour length, $\Lambda = L_c/L_p$ is a reduced, dimensionless, contour length, and L_p is the persistence length. The coefficients A_i involve a similarly defined reduced diameter ($d_c/(2L_p)$), where d_c is the chain diameter. The parameters $L_c = 2.8 \times 10^3$ nm and $d_c = 1.0$ nm were estimated using the molecular weight and amino acid content for PGM (Fiebrig et al., 1995; Allen, 1981). By using Eq. 8 to analyze the D values at pH 7 we obtain $L_P = 8.5$ nm, which is slightly smaller than $L_P = 14.5$ nm obtained by Shogren et al. (1989) for ovine submaxillary mucin (OSM) at pH 7. In contrast to this, a significantly larger persistence length, $L_P = 43$ nm, is obtained using Eq. 8 for the D values measured for PGM at pH 2.0.

We also estimate the average end-to-end distance (Yamakawa, 1971):

$$\langle R^2 \rangle = 2L_cL_p - 2L_p^2[1 - \exp(-L_c/L_p)],$$
(9)

as 490 nm for PGM at pH 2.

If a rodlike model (Riseman and Kirkwood, 1950) is used,

$$D = \frac{kT}{3\pi\eta L} \ln(L/d), \tag{10}$$

$$D_R = \frac{3kT}{\pi\eta L^3} \ln(L/d), \tag{11}$$

where L and d denote the length and diameter of the rod. Equations 10 and 11 give $L = 390$ nm and $d = 55$ nm for PGM at pH 2. The dimensions obtained by either model are in excellent agreement with the range of lengths seen in transmission electron microscopy studies (Fiebrig et al., 1995).

Dynamic light scattering at high concentrations

At high PGM concentrations (≥ 10.0 mg/ml), $S(q, t)$ for PGM solution no longer follows an exponential decay; its actual form is pH-dependent. When we analyzed the data by CONTIN we obtained numerous overlapping peaks in the distribution of relaxation times. The plot of $\log[-\ln(S(q, t))]$ versus $\log(t)$ for PGM solution at 10.0 mg/ml and pH 7.0 shows two distinct decay characteristics, as illustrated in Fig. 4. The linearity of this plot at late times indicates that $S(q, t)$ takes the form of a stretched exponential decay in the time range 10^2-10^4 μs. By comparing with the similar observation of a stretched exponential decay in $S(q, t)$ in pre-gel solutions of synthetic polymers (Adam et al., 1988; Martin and Wilcoxon, 1988; Martin et al., 1991; Fang et al., 1991; Nystrom and Lindman, 1995; Konak et al., 1996), we conclude that at 10.0 mg/ml and pH 7.0, PGM forms polydisperse, partially penetrating aggregates that are still in a solution. The observed exponent, $\beta = 0.39$, is comparable to those found in synthetic polymer solutions, where $\beta = 0.45$ has been seen for associating branched polymethyl-methacrylate in the Θ-solvent 4-heptanone (Konak et al., 1996), and $\beta = 0.26$ for the same polymer in a good solvent, butylacetate (Fang et al., 1991).

The data shown in Fig. 4 were fit according to Eq. 4 to extract the decay rates Γ_i (i = c or s) corresponding to the cooperative and slow cluster dynamics, respectively. Fig. 5 shows the q-dependence of Γ_i (i = c or s) from DLS measurements of PGM solution 10.0 mg/ml pH 7.0 at different scattering angles. For both the cooperative and the slow cluster dynamics, instead of the usual q^2-dependence, we obtained $\Gamma_i \sim q^{a_i}$, where the exponents are >2: $a_c = 3.0$ and $a_s = 3.9$. The observation that the q-dependence of the slow mode is significantly stronger than the usual q^2-dependence is in agreement with a number of studies on associating polymer systems (Konak et al., 1996; Nystrom et al., 1993), and both physical (Ren et al., 1992; Ren and Sorensen, 1993; Nystrom and Lindman, 1995) and chemical gels in pre-gel states (Martin et al., 1991).

The observed scaling of $\Gamma_c \sim q^3$ can be explained by the Zimm model (Zimm, 1956) for polymer chain dynamics, which takes into account additional hydrodynamic interactions between the segments in one macromolecular chain. The strong q-dependence of the slow mode may be at least qualitatively explained by the coupling theory (Ngai, 1992) which deals with the problem of how the relaxation of a specific cluster is "slowed down" because of the coupling to other clusters in its complex surroundings.

For a PGM solution of 10.0 mg/ml at pH 2.0, neither the CONTIN analysis nor the stretched exponential decay can be used to describe the $S(q, t)$ function appropriately. The profile of the long-term tail of $S(q, t)$ becomes a power-law decay function in the time range $t = 10^3$-10^6 μs, as shown in Fig. 6. An exponent $\Phi = 0.34$ is obtained by using Eq. 5 to analyze the $S(q, t)$ function. The observed exponent $\Phi = 0.34$ is close to the value $\Phi = 0.34$ for silica gels (Martin and Wilcoxon, 1988), $\Phi = 0.35$ for PMMA gels in the Θ-solvent 4-heptanone (Konak et al., 1996), and $\Phi = 0.27$
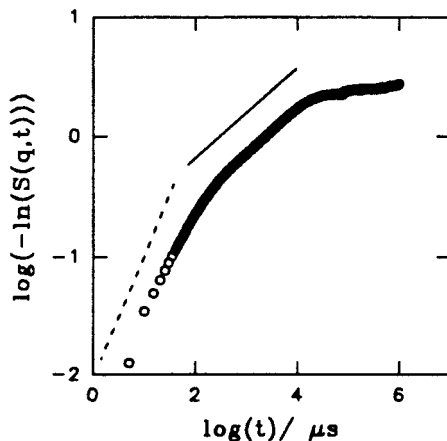

FIGURE 4 Plot of $\log[-\ln(S(q, t))]$ versus $\log(t)$ for PGM solution of 10.0 mg/ml, pH 7.0. The dashed line corresponds to a single exponential decay while the solid line corresponds to a stretched exponential decay with $\beta = 0.39$ (see Eq. 4).
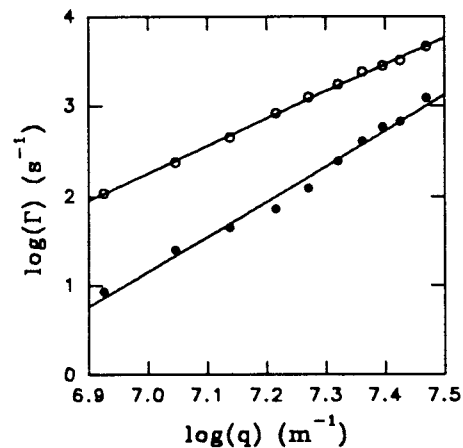

FIGURE 5 The q-dependence of cooperative (Γ_c, ○) and slow (Γ_s, ●) decay rates for PGM solution of 10.0 mg/ml, pH 7.0. The data scales as $\Gamma_i \sim q^{a_i}$ (i = c or s) with exponents $a_c = 3.0$ and $a_s = 3.9$.
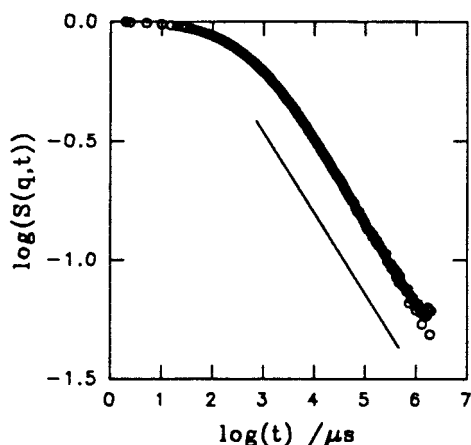
FIGURE 6 Plot of log[$S(q, t)$] versus log(t) for PGM of 10.0 mg/ml, pH 2.0. The solid line corresponds to a power-law decay with $\Phi = 0.34$ (see Eq. 5).

for the same gels in the good solvent butylacetate (Fang et al., 1991). At shorter times there is a contribution from an exponential decay, most likely related to the collective mode of gel dynamics (Tanaka et al., 1973). In a well-gelled sample, far from the gel point a fast exponential decay corresponding to the decay of concentration fluctuations on length scales comparable to the correlation length in the gel is usually observed. We were not able to investigate the well-gelled regime in PGM, because at the high concentrations needed to produce a strongly gelled state the samples were very turbid, and thus not suitable for DLS measurements.

In synthetic polymers a transition of the $S(q, t)$ function from a stretched exponential decay to a power-law decay signals the change in relaxation dynamics occurring at a sol-gel transition. Therefore, Figs. 4 and 6 demonstrate that PGM at 10.0 mg/ml undergoes a pH-dependent sol-gel phase transition: at pH 7.0 PGM is a solution of partially penetrating aggregates, whereas at pH 2.0 PGM is a gel in the vicinity of a gel point. Such a pH-induced sol-gel transition is in excellent agreement with our previous studies on the PGM solution's viscosity, which showed a dramatic increase in the viscosity as the pH was decreased to below 5 (Bhaskar et al., 1991). As mentioned earlier, the sol-gel transition indicated by the change of $S(q, t)$ function from stretched exponential decay to power-law decay is commonly seen in synthetic polymer systems; however, to our knowledge this is the first time that such a transition in dynamics has been correlated to a physiologically relevant gelation process.

Role of hydrophobic interactions in the gelation of PGM

It is reasonable to assume that the conformational change of PGM macromolecules and the sol-gel transition of PGM solution are correlated, since both of them show similar pH-dependence. The PGM macromolecule, like most members of the mucin family, consists of alternating hydropho-

bic and hydrophilic portions in its primary structure (Allen, 1981; Bansil et al., 1995; Fiebrig et al., 1995), therefore its extended conformation at low pH would expose the hydrophobic regions. To avoid unfavorable contact with water molecules (the solvent), these hydrophobic regions would form intermolecular domains if the solution is concentrated enough, thus forming a PGM gel at low pH with hydrophobic domains acting as cross-links. We have observed that at pH 2 the viscosity of PGM solution containing CHAPS ((3-[(3-cholamidopropyl)dimethylammonio]-1-propane-sulfonate), a zwitterionic detergent, is considerably less than that of PGM solution alone, indicating that hydrophobic interactions may be responsible in part for the pH-dependent increase in PGM viscosity.

To further examine whether there are pH-dependent changes in the exposure of such hydrophobic sites of PGM, we carried out binding studies with the fluorescent probes ANS and NPNA. At an excitation wavelength of 365 nm, a dilute aqueous solution of ANS (3.2×10^{-5} M) has relatively low fluorescence with an emission maximum at ~520 nm. Upon incubation with PGM (1.0 mg/ml, pH 7.0), the emission maximum of ANS is shifted to 480 nm and the fluorescence intensity is increased significantly compared to that of ANS alone. The shift of the emission maximum to lower wavelength and increase in relative fluorescence are both indicative of ANS binding to PGM. At pH 4.0 and below, the fluorescence intensity becomes considerably higher, and at pH 2.0 there is a 10-fold increase in relative fluorescence, as shown in Fig. 7. Under the same conditions, the fluorescence intensity of ANS alone was unaffected by pH (not shown). This enhancement of ANS fluorescence is lost upon proteolytic treatment of PGM, indicating that the hydrophobic binding sites are on the protease-susceptible nonglycosylated portions of the PGM molecule. This increased fluorescence is lost upon changing the pH from 2.0 to 7.0 and can be restored by bringing the pH back to 2.0, indicating that the pH-dependent changes are reversible and not the result of irreversible denaturation of PGM at low pH.

The addition of salt does not affect the fluorescence at pH 2.0, but results in a slight increase in fluorescence at pH 7.0, as shown in Fig. 8. Because ANS and PGM are both negatively charged, charge repulsion in the presence of salt will no longer be effective; this may explain why the addition of salt increases fluorescence at pH 7.0. However, at pH 7.0 the increase in fluorescence (and thus binding) resulting from added salt up to 1.0 M is still far below that observed at pH 2.0. Thus charge repulsions alone are not responsible for the marked increase in fluorescence at pH 2.0, and exposure of hydrophobic sites through a conformational change may also be occurring.

ANS binding to PGM was studied at several temperatures ranging from 25 to 55°C. At pH 7 and pH 4, the fluorescence is practically unchanged, whereas at pH 2 there is a slight progressive increase in relative fluorescence with increasing temperature. This indicates that the binding is stable at temperatures considerably higher than ambient and
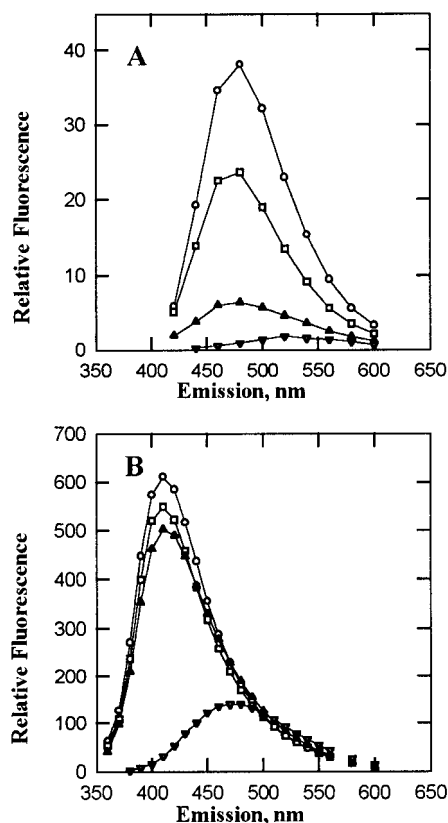
FIGURE 7 pH dependence of PGM binding to fluorescence probes. ▽, Fluorescence probe alone at pH 7; ▼, fluorescence probe + PGM at pH 7; ●, at pH 4; ○, at pH 2. (A) Relative fluorescence of ANS + PGM solution at different pH values. (B) Relative fluorescence of NPNA + PGM solution at different pH values. The weak emissions of the probes are enhanced upon incubation with PGM with a shift of the emission maximums to lower wavelengths. There are marked increases in relative fluorescence intensities with decreasing pH. The shift of the emission maximum to lower wavelength and increase in relative fluorescence are both indicative of binding.
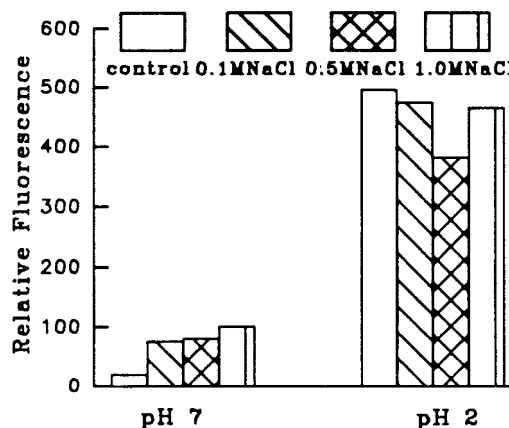

FIGURE 8 The effect of added salt on the binding of ANS + PGM solution. Salt concentration has little effect on the relative fluorescence of ANS + PGM solution at pH 2.

matically decreases PGM viscosity (Bhaskar et al., 1991), suggests that the conformational change is partially mediated by electrostatic interactions. Amino acid residues with $pK_a \approx 4$, Glu and/or Asp, may be involved in the conformational change and the subsequent sol-gel transition processes, since both of these changes occur at pH $\approx$ 4. Thus a region rich in hydrophobic residues bounded by charged amino acid residues would favor formation of such cross-links at high concentration and low pH (pH $\leq$ 4), as demonstrated in Fig. 9. We have recently isolated a partial cDNA clone encoding a Cys-rich region of PGM (Bhaskar et al., unpublished results). Interestingly, the peptide translated by this clone has in its sequence amino acid regions

thus is of relevance under in vivo temperature of 37°C. The increase in fluorescence with increasing temperature observed at pH 2 further supports the notion that the binding is hydrophobic in nature.

PGM at the same concentration also markedly enhances the relative fluorescence of the uncharged probe, NPNA. At an excitation wavelength of 342 nm, NPNA (3.2×10^{-5} M) has a fluorescence emission with a maximum at 480 nm. Incubation with mucin solution at pH 7 shifts the emission maximum to 410 nm with a fourfold increase in intensity. There is a progressive increase in PGM-induced fluorescence intensity of NPNA with decreasing pH, further supporting the hypothesis of a pH-induced conformational change.

Role of electrostatic interactions in the gelation of PGM

The fact that the PGM solution's viscoelastic properties are reversible upon changing pH, and high ionic strength dra-
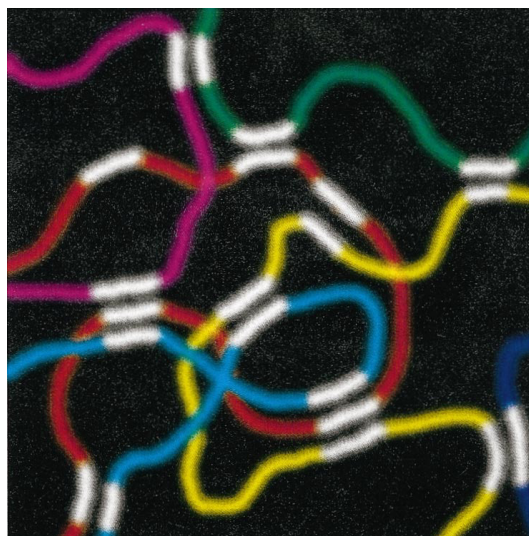

FIGURE 9 A sketch showing the gelation of PGM solution at high concentration and low pH. Different colors are used to show individual PGM macromolecules. In its extended conformation, the PGM macromolecule exposes its hydrophobic regions (*white segments*), which form intermolecular hydrophobic domains to cross-link PGM macromolecules. In this two-dimensional representation, the conformation in some cases may appear less extended than it actually is in three dimensions.

high in hydrophobic residues bounded by Asp (or Glu) and Arg, and thus could potentially form such a hydrophobic loop that can open to expose its hydrophobic interior when the pH is decreased below pH 4.

Is the pH-dependent transition unique to PGM?

As has already been mentioned, PGM has a larger persistence length at pH 2 (43 nm) than at pH 7 (8 nm). The question arises whether this conformational transition is unique to PGM. Light scattering data on ovine submaxillary mucin (Shogren et al., 1989) gave its persistence length at pH 7 as 14.7 nm. Since no measurements were made at lower pH one cannot say if OSM would also be stiffer at lower pH. To shed further light on this question, we examined GBM, which has size and molecular weight similar to PGM. In the range of concentrations ≤5.0 mg/ml, the average diffusion coefficient of GBM was found to be $D = 5.2 \times 10^{-8}$ cm^2/s. At concentrations ≥10.0 mg/ml, $S(q, t)$ showed stretched exponential decay at both pH 7.0 and pH 2.0, with slightly different values of the stretched exponential's exponent (β) and the q-dependence's exponents (a_c and a_s) as compared to PGM (cf. Fig. 4 and Fig. 5). At 10.0 mg/ml and pH 7.0 $a_c = 3.0$, $a_s = 5.5$, and $\beta = 0.24$; at 10.0 mg/ml and pH 2.0 $a_c = 3.0$, $a_s = 3.8$, and $\beta = 0.40$, as shown in Fig. 10. However, neither conformational change nor power-law decay behavior was observed for all the GBM solutions examined (0.25–10.0 mg/ml, pH 7.0 and 2.0), indicating that GBM does not form a gel under any of the conditions mentioned above, but exists as a viscous solution of aggregates. Although GBM also contains a Cys-rich region (Nunes et al., 1995), which is able to interact hydrophobically with biliary lipids and is important for polymerization, this domain does not appear to be pH-sensitive in the same manner as was found in PGM. Binding studies also show that the relative increase in fluorescence intensity upon incubating with GBM is much less than that

incubated with PGM (Smith and LaMont, 1984). Physiologically, the pH of the gallbladder rarely falls below 6.5; a gel in the gallbladder might promote gallstone formation and is thus undesirable (Afdhal et al., 1995).

Extended, rodlike molecules often exhibit liquid crystalline order. For example, slug mucin has been shown to have nematic liquid crystalline phases (Viney et al., 1993). Although no studies of liquid crystallinity in PGM have been reported in the literature, our previous observation of highly dendritic viscous fingers in PGM solution (Bhaskar et al., 1992) is consistent with the effects of flow-induced ordering of anisotropic molecules, since dendritic fingers have been observed in anisotropic solutions (Horvath et al., 1987).

CONCLUSIONS

In conclusion, we have demonstrated, in vitro, that PGM undergoes a pH-induced conformational change that results in a sol-gel phase transition of mucin at higher concentrations. Dye-binding studies strongly suggest that the cross-links of the mucin gel are due to intermolecular, hydrophobic interactions.

In this work we have examined the role of changing pH on properties of mucin solutions. The mucin in gastric mucus is in a more complex milieu, and other factors may also play a role in the protection mechanism. Based on our in vitro studies of conformational change, gelation, and viscous fingering we suggest the following plausible scenario of how changes in pH could lead to a sol-gel transition in the mucus layer and prevent the stomach from being digested by its own secretion. Before HCl is secreted, gastric mucin macromolecules are random coils at pH 6–7 and the mucus layer is a viscous solution. The pH is maintained by bicarbonate ions secreted by the gastric epithelium (Flemstrom, 1987). HCl secreted from the gastric glands has been shown to pass through the mucus layer in restricted areas (Holm and Flemstrom, 1990), which may have the physical features of a jet-like viscous finger (Bhaskar et al., 1992). The pH-induced conformational change described in this paper would transform the gastric mucin macromolecules in contact with the acid jet to an extended wormlike or rodlike conformation. At the high concentrations of mucin typically found in the stomach mucus, the mucus layer in the vicinity of this acid jet would undergo a sol-gel transition to form a gel, cross-linked by intermolecular hydrophobic domains. This gel provides a physical barrier (like the walls of a tubing) at the limits of the channel where the HCl contacts the gastric mucin macromolecules, thus preventing the mucus layer from being grossly acidified. The gelated gastric mucin resists diffusion of acid, and preserves the pH gradient of the mucus layer (pH 2 at the lumen to pH 7 at the apical cell surface). In other words, the back diffusion of gastric acid is prevented, and the stomach is protected against being digested by the gastric acid. Finally, we also note that DLS provides a sensitive probe of mucin structure and aggregation and could be used to assess the
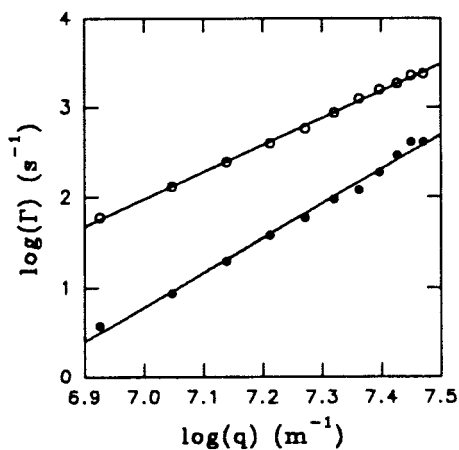

FIGURE 10 The q-dependence of cooperative (Γ_c, ○) and slow (Γ_s, ●) decay rates for GBM solution of 10.0 mg/ml, pH 2.0. The data scales as $\Gamma_i \sim q^{i}_a$ (i = c or s) with exponents $a_c = 3.0$, $a_s = 3.8$.

role of other factors that may be involved in the answer to this profound question in physiology.

REFERENCES

Adam, M., M. Delsanti, J. P. Munch, and D. Durand. 1988. Dynamical studies of polymeric cluster solutions obtained near the gelation threshold: glasslike behavior. *Phys. Rev. Lett.* 61:706–709.

Afdhal, N. H., N. Niu, D. P. Nunes, R. Bansil, X. Cao, D. Gantz, D. M. Small, and G. D. Offner. 1995. Mucin-vesicle interactions in model bile: evidence for vesicle aggregation and fusion prior to cholesterol crystal formation. *Hepatology.* 22:856–865.

Allen, A. 1981. Structure and function of gastrointestinal mucus. *In* Physiology of the Gastrointestinal Tract, 1st ed. L. R. Johnson, editor. Raven Press, New York. 617–639.

Allen, A., and A. Garner. 1980. Gastric mucus and bicarbonate secretion and their possible role in mucosal protection. *Gut.* 21:249–262.

Bansil, R., H. E. Stanley, and J. T. LaMont. 1995. Mucin Biophysics. *Annu. Rev. Physiol.* 57:635–657.

Bell, A. E., L. A. Sellers, A. Allen, J. M. Cunliffe, E. R. Morris, and S. B. Ross-Murphy. 1982. Properties of gastric and duodenal tract and their ability to lubricate. *Am. J. Physiol.* 244:G645–G651.

Berne, B. J., and R. Pecora. 1976. Dynamic Light Scattering with Application to Chemistry, Biology, and Physics. Wiley Interscience, New York.

Bhaskar, K. R., P. Garik, B. S. Turner, J. D. Bradley, R. Bansil, H. E. Stanley, and J. T. LaMont. 1992. Viscous fingering of HCl through gastric mucin. *Nature.* 360:458–461.

Bhaskar, K. R., D. Gong, R. Bansil, S. Pajevic, J. A. Hamilton, B. D. Turner, and J. T. LaMont. 1991. Profound increase in viscosity and aggregation of pig gastric mucin at low pH. *Am. J. Physiol.* 261:G827–G832.

Brown, W., and T. Nicolai. 1993. Dynamic properties of polymer solutions. *In* Dynamic Light Scattering. W. Brown, editor. Clarendon Press, Oxford, U.K.

Cao, X. 1997. Aggregation and gelation of mucin and its interactions with lipid vesicles. Ph.D. dissertation, Boston University.

Carlstedt, I., H. Lindgren, and J. K. Sheehan. 1983. The macromolecular structure of human cervical mucus glycoproteins. *Biochem. J.* 213:427–435.

Chu, B. 1991. Laser Light Scattering. Basic Principles and Practice, 2nd ed. Academic Press, Boston.

Fang, L., W. Brown, and C. Konak. 1991. Dynamic light scattering study of the sol-gel transition. *Macromolecules.* 24:6839–6842.

Fiebrig, I., S. E. Harding, A. J. Rowe, S. C. Hyman, and S. S. Davis. 1995. Transmission electron microscopy studies on pig gastric mucin and its interactions with chitosan. *Carbohydr. Polym.* 28:239–244.

Flemstrom, G. 1987. Gastric and duodenal mucin bicarbonate secretion. *In* Physiology of the Gastrointestinal Tract, 2nd ed. L. R. Johnson, editor. Raven Press, New York. 1011–1029.

Gong, D., B. S. Turner, K. R. Bhaskar, and J. T. LaMont. 1990. Lipid binding to gastric mucin: protective effect of oxygen radicals. *Am. J. Physiol.* 259:G681–G686.

Heatley, N. G. 1959. Mucosubstance as a barrier to diffusion. *Gastroenterology.* 37:313–318.

Hollander, F. 1954. Two-component mucous barrier: its activity in protecting gastroduodenal mucosa against peptic ulceration. *Arch. Intern. Med.* 93:107–120.

Holm, L., and G. Flemstrom. 1990. Microscopy of acid transport at the gastric surface in vivo. *J. Int. Med.* 228:91–95.

Horvath, V., T. Vicsek, and J. Kertesz. 1987. Viscous fingering with imposed uniaxial anisotropy. *Phys. Rev. A.* 35:2353–2356.

Konak, C., L. Mrkviekova, and R. Bansil. 1996. Dynamics of pre-gel solutions and gels in a theta solvent near a spinodal. *Macromolecules.* 29:6158–6164.

Martin, J. E., and J. P. Wilcoxon. 1988. Critical dynamics of the sol-gel transition. *Phys. Rev. Lett.* 61:373–376.

Martin, J. E., J. P. Wilcoxon, and J. Odinek. 1991. Decay of density fluctuations in gels. *Phys. Rev. A.* 43:858–872.

Ngai, K. L. 1992. Interpretation of dynamical properties of polymeric cluster solutions. *In* Structure and Dynamics of Strongly Interacting Colloids and Supramolecular Aggregates in Solutions. NATO ASI Series C, Vol. 369. S. H. Chen, J. S. Huang, and P. Tartaglia, editors. Kluwer Academic Publishers, Dordrecht, The Netherlands.

Nunes, D. P., A. C. Keates, N. H. Afdhal, and G. D. Offner. 1995. Isolation and identification of a unique bovine gallbladder mucin clone. *Biochem. J.* 310:41–48.

Nystrom, B., and B. Lindman. 1995. Dynamic and viscoelastic properties during the thermal gelation process of a nonionic cellulose ether dissolved in water in the presence of ionic surfactants. *Macromolecules.* 28:967–974.

Nystrom, B., H. Walderhaug, and F. K. Hansen. 1993. Dynamic crossover effect observed in solutions of a hydrophobically associating water-soluble polymer. *J. Phys. Chem.* 97:7743–7752.

Pfeiffer, C. 1981. Experimental analysis of hydrogen ion diffusion in gastrointestinal mucus glycoprotein. *Am. J. Physiol.* 240:G176–G182.

Provencher, S. W., J. Hendrix, L. DeMaeyer, and N. Paulussen. 1978. Direct determination of molecular weight distributions of polystyrene in cyclohexane with photon correlation spectroscopy. *J. Chem. Phys.* 69:4273–4276.

Ren, S. Z., W. F. Shi, W. B. Zhang, and C. M. Sorensen. 1992. Anomalous diffusion in aqueous solutions of gelatin. *Phys. Rev. A.* 45:2416–2422.

Ren, S. Z., and C. M. Sorensen. 1993. Relaxations in gels: analogies to α and β relaxations in glasses. *Phys. Rev. Lett.* 70:1727–1730.

Riseman, J., and J. G. Kirkwood. 1950. The intrinsic viscosity, translational and rotatory diffusion constants of rod-like macromolecules in solution. *J. Chem. Phys.* 18:512–516.

Shogren, R., T. A. Gerken, and N. Jentoft. 1989. Role of glycosylation on the conformation and chain dimensions of O-linked glycoproteins: light scattering studies of ovine submaxillary mucin. *Biochemistry.* 28:5525–5536.

Smith, B. F., and J. T. LaMont. 1984. Hydrophobic binding properties of bovine gallbladder mucin. *J. Biol. Chem.* 259:12170–12177.

Strous, G. J., and J. Dekker. 1992. Mucin-type glycoproteins. *Crit. Rev. Biochem. Mol. Biol.* 27:57–92.

Tanaka, T., L. O. Hocker, and G. B. Benedek. 1973. Spectrum of light scattered from a viscoelastic gel. *J. Chem. Phys.* 59:5151–5159.

Viney, C., A. E. Huber, and P. Verdugo. 1993. Liquid crystalline order in mucus. *Macromolecules.* 26:852–855.

Williams, S. E., and L. A. Turnberg. 1980. Retardation of acid diffusion by pig gastric mucus: a potential role in mucosal protection. *Gastroenterology.* 79:299–304.

Yamakawa, H. 1971. Modern Theory of Polymer Solutions. Harper and Row, New York.

Yamakawa, H., and M. Fujii. 1973. Translational friction coefficient of worm-like chains. *Macromolecules.* 6:407–415.

Zimm, B. H. 1956. Dynamics of polymer molecules in dilute solution: viscoelasticity, flow birefringence and dielectric loss. *J. Chem. Phys.* 24:269–278.